Civil and Environmental Engineering
Vol. 19, Issue 1, 288-300, DOI: 10.2478/cee-2023-0026

ASSESSMENT OF SLOPE STABILITY WITH THE ASSISTANCE OF ARTIFICIAL NEURAL NETWORK AND DIFFERENTIAL EVOLUTION

Vu Truong VU[1,*]

[1] Faculty of Civil Engineering, Nguyen Tat Thanh University 300A, Nguyen Tat Thanh, Ward 13, District 4, Ho Chi Minh City, Viet Nam.
[*] corresponding author: vutruongvu@gmail.com

Abstract

This study aims for two purposes: firstly, using the Differential Evolution method combined with limit equilibrium methods to find the factor of safety of a variety of different configurations of slopes and soil parameters. Two patterns of the embankments are assessed, a one-layer soil pattern with 540 cases and a two-layer soil pattern with 24300 cases. Secondly, using these data to train and test an artificial neural network for predicting the factor of safety of slopes. The experimental data and values predicted by the artificial neural network correlate well with a linear coefficient of correlation of around 0.99. Given large enough training data, the proposed approach shows its reliability in quick evaluation of the slope stability without a long process of searching for a critical slip surface.

Keywords:

Slope stability;
Differential evolution;
Artificial neural network;
Optimization;
Limit equilibrium method.

1 Introduction

Slope stability has been studied by many methods, e.g. limit equilibrium methods such as Fellenius' ordinary method [1] and Bishop's simplified method [2] are used commonly for their simplicity and acceptable accuracy in practice. Later, heuristic methods are utilized to find the minimum factor of safety which is formulated as the objective function of variables expressing the radius and center coordinates of the slip circle. For instance, the use of genetic algorithms in [3, 4], ant colony optimization in [5], particle swarm optimization in [6, 7], and differential evolution in [7]. Normally, the slope stability is evaluated for a given data of the embankment and soil through a process of analysis using limit equilibrium methods (or other methods) and searching to find the critical slip surface. Recently, with the assistance of the artificial neural network (ANN), one can predict the slope stability via the trained ANN without searching directly for the critical slip surface and its corresponding factor of safety, e.g. using ANN for slopes in homogeneous soil [8], or in two-layer purely cohesive soil slopes [9]. Later, other machine learning methods are also used for slope stability, e.g. the support vector machine and its version with the stability status that has been modeled as a classification problem [10, 11]

However, the above studies only surveyed small data on slope configurations, and most of the data are for slopes with homogeneous soil. This study will extend the application of ANN for both one-layer and two-layer soil slopes with a variety of slope configurations and soil parameters. The next parts of the article are structured as follows. Section 2 describes briefly a few limit equilibrium methods in the assessment of slope stability. Section 3 introduces differential evolution as an optimization technique for finding the critical slip surface. Section 4 describes briefly the artificial neural network and the model used in this study. Section 5 formulates the problem of searching for the critical slip surface and data preparation for ANN performance. Then sections 6 and 7 are for results and conclusions, respectively.

2 Assessment of slope stability using limit equilibrium methods

This study uses two common limit equilibrium methods (LEM), namely Fellenius' ordinary method [1] and Bishop's simplified method [2]. These methods assume a circular slip surface and the corresponding factor of safety *FS* is evaluated by calculation forces acted on slices of the slip area. For simplicity, Fellenius' ordinary method neglects interaction forces *E* and *T* between sides of the slide, Fig. 1, while Bishop's simplified method neglects only the interaction force *T*. Factor of safety *FS* are given in equation (1) for Fellenius' ordinary method and equation (2) for the Bishop's simplified method:

$$FS = \frac{\sum_1^n (c_i l_i + W_i \cos\alpha_i tg\varphi_i)}{\sum_1^n W_i \sin\alpha_i}, \tag{1}$$

$$FS = \frac{\sum_1^n (c_i l_i + \frac{W_i \mathrm{tg}\varphi_i}{\cos\alpha_i})(1 + \frac{\mathrm{tg}\varphi_i \mathrm{tg}\alpha_i}{FS})^{-1}}{\sum_1^n W_i \sin\alpha_i}, \tag{2}$$

where:
n - number of slices,
n - number of slices,
l_i - the length of the i^{th} slice base,,
c_i - the stress cohesion of the i^{th} slice,
φ_i - the angle of internal friction of the i^{th} slice,
W_i - the weight of the i^{th} slice,
α_i - the angle between the normal force on the base of the i^{th} slice and the vertical direction.

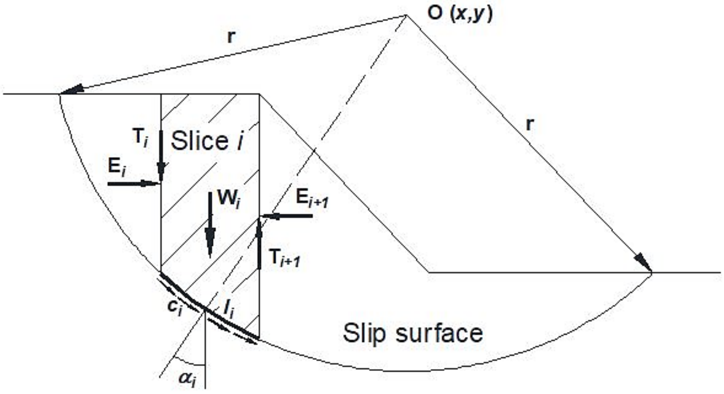

Fig. 1: Forces acting on slices of a circular slip surface.

3 Differential evolution

Differential evolution (DE) is a population-based algorithm [12] that uses mutation, crossover, and selection operators to self-adjust the search direction during finding the best solution. For a minimization problem, these operators are defined as follows.

- Mutation

$$v_{i,G+1} = x_{r1,G} + FM(x_{r2,G} - x_{r3,G}) \text{ , } I = 1, 2, ...Npop, \tag{3a}$$

or

$$v_{i,G+1} = x_{best,G} + FM(x_{r1,G} + x_{r2,G} - x_{r3,G} - x_{r4,G}) \text{ , } I = 1, 2, ...Npop, \tag{3b}$$

where, G is the current generation; $Npop$ is the population size, $v_{i,G+1}$ is a mutant vector; $x_{best,G}$ is the best vector; r_1, r_2, r_3, r_4 are random integer numbers, mutually different in [1, $Npop$] and different from the running index I; FM is the mutation constant in (0, 2);

- Crossover

$$u_{i,G+1} = (u_{1i,G+1}, u_{2i,G+1}, \ldots, u_{Di,G+1}), \tag{4}$$

with

$$u_{ji,G+1} = \begin{cases} v_{ji,G+1} & \text{if } (r \leq CR) \text{ or } j = k \\ x_{ji,G} & \text{if } (r > CR) \text{ and } j \neq k \end{cases}, \quad j = 1, 2, ...D,$$

where, r is a random number in (0, 1), CR is the crossover constant in [0, 1], D is the dimension of the problem, and k is a random integer number in [1, D].

- Selection

$$x_{i,G+1} = \begin{cases} u_{i,G+1} & \text{if } f(u_{i,G+1}) < f(x_{i,G}) \\ x_{i,G} & \text{otherwise} \end{cases}, \tag{5}$$

where f is the objective function.

The algorithm initially starts with a random population, then uses these operators for searching the “optimal” solution. The search stops when it satisfies a given stopping criterion, i.e. number of iterations or convergence criteria. An illustration of a minimization problem using differential evolution is given in Fig. 2.

```
For i = 1, N
   For j = 1, D
      Initialize random values xji,G
   End For
   Evaluate objective function, f(xi,G)
End For
Repeat
   For i = 1, N
      Generate 3 integer random numbers
          r1 ≠ r2 ≠ r3 ≠ i ∈ [1, N]
      Generate integer random number k ∈ [1, D]
      For j = 1, D
         Generate random number r ∈ (0,1)
         If ((r ≤ CR) or (j = D)) then
            uki,G+1 = xkr1,G + FM(xkr2,G − xkr3,G)
         Else
            uki,G+1 = xki,G
         End If
         k = (k + 1) modulo D
      End For
      Evaluate objective function, f(ui,G+1)
      If f(ui,G+1) < f(xi,G) then
         xji,G+1 = uji,G
      Else
         xji,G+1 = xji,G
      End If
   End For
   For i = 1, N
      For j = 1, D
         Update xji,G = xji,G+1
      End For
   End For
Until stopping criterion is met.
```

Fig. 2: Differential evolution algorithm for a minimization problem.

4 Artificial neural network

The artificial neural network is an algorithm that tries to mimic the human brain. Its original ideas started in the 1940s and becomes popular in the 1980s with the main representative being the multilayer perceptron model trained by the backpropagation learning algorithm [13]. The ANN architecture in this study, shown in Fig. 3, consists of an input layer, hidden layer(s) and an output layer. Each layer consists of neurons (or nodes). A bias node with a value of 1 is added to each layer to shift the activation function. Connections between neurons in layers are expressed as weights which are determined by a training process. In this study, the sigmoid activation function (as eq. 6) is applied to transfer the values between neurons of layers, and the gradient descent method is adopted in the backpropagation learning algorithm.

The number of neurons in the input layer depends on the embankment pattern. It consists of 5 neurons represented for h, m, γ_1, c_1, and φ_1 for one-layer soil cases, and 8 neurons represented for h, m, γ_1, c_1, φ_1, γ_2, c_2, and φ_2 for two-layer soil cases. The output layer is a single neuron estimating the factor of safety (*FS*) of the slope. The reasonable number of hidden layers and neurons in each hidden layer will be determined by experiments regarding the balance between the result quality and the running time. After trials with different scenarios, this study uses one hidden layer with 5 neurons for the one-layer soil pattern, and two hidden layers with 5 neurons in each layer for the two-layer soil pattern. Similarly, the learning rate in the gradient descent method is chosen as 0.01 for one-layer soil cases and 0.001 for two-layer soil cases.

The training and testing samples are 80 % and 20 % of the total data of each case, respectively. The training process is iterated to minimize the mean squared error between the predicting outputs and the target values (actual values). The maximum epoch is set to 300000. Initial weights with a mean of zero are chosen randomly within the range [-1, 1]. Details of these parameters are listed in Table 1.

$$\phi(x) = \frac{1}{1+e^{-\beta x}}. \tag{6}$$

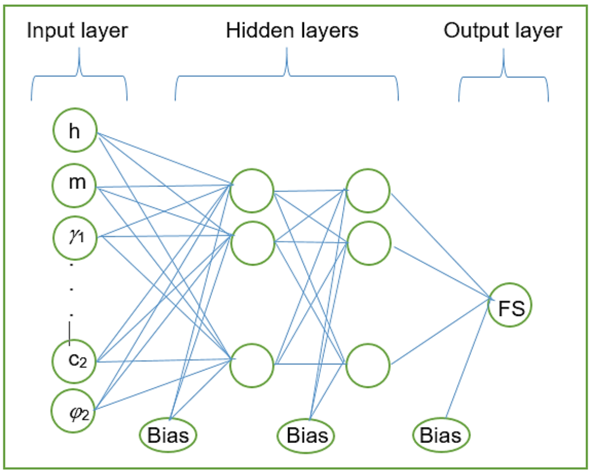

Fig. 3: ANN architecture in this study.

Table 1: Parameters of the ANN models.

Parameters	One-layer soil	Two-layer soil
Number of input nodes	5	8
Number of hidden layers	1	2
Number of hidden nodes	5	5 for each hidden layer
Number of output nodes	1	1
Activation function	Sigmoid function $\phi(x) = \frac{1}{1+e^{-\beta x}}$	
Optimizer	Gradient descent method	
Maximum iteration	300000	
Learning rate	0.01	0.001

5 Problem formulation

5.1 Searching for the critical slip surface

For a given configuration of an embankment, the critical slip surface gives the minimum safety factor of the slope. The critical slip surface is assumed as a circle in limit equilibrium methods. It is defined by three parameters, namely the center coordinates (*x, y*) and radius *r* of the circle, which are the solution to the problem formulated as follows:

- Minimize *FS* = Factor of safety of the slope calculated by the equation (1) or (2).
- Subject to - Kinematic constraints to ensure a reasonable trial circular slip.
  - Bounds of three design variables.

$x_{min} \le x \le x_{max}$, $y_{min} \le y \le y_{max}$, $r_{min} \le r \le r_{max}$,

where: x, y, and r are the center coordinates and radius of the circular slip surface, (x_{min}, y_{min}), (x_{max}, y_{max}) are the bottom left and the top right corners of a rectangle predicted to contain the center of circular slip surfaces, (r_{min}, r_{max}) ensures the radius of slip circles is within a reasonable limit.

The differential evolution algorithm showed its ability in searching for the optimal solution to this problem [7]. Therefore, we will choose similar parameters of DE in this study, i.e. the population *Npop* = 30, number of iterations *Iter* = 50, the mutation constant *FM* = 0.5, and the crossover constant *CR* = 1.0.

5.2 Data preparation for ANN

For effective training and testing of the ANN, we need to prepare large enough data of critical surfaces in a variety of embankment configurations. In this study, we choose two patterns of the embankments, one with a one-layer soil, Fig. 4a, and one with a two-layer soil, Fig. 4b. Parameters include slope height h, slope ratio m, unit weight γ, cohesion c, and internal friction angle φ. For simplicity, the pore pressure ratio is assumed zero in this study. The bounds and increment of parameters are detailed in Table 2, e.g. the slope height h is from 3 m to 6 m with an increment of 1 m, the slope ratio m varies from 1 to 2 with an increment of 0.5, and similarly for other parameters. Consequently, the total number of assessments of the slope stability used as data for ANN is 540 for the one-layer soil and 24300 for the two-layer soil.

The study has assessed the safety factor of all the above slope configurations. For each case, the factor of safety and the corresponding circular slip surface are recorded in a database. From the assessment, ranges of the factor of safety by Fellenius' and Bishop's methods for the two patterns are summarized in Table 2. Examples of some results of slope stability used as training and testing data are given in Table 3.

As a large variance among ranges of the input parameters, it is necessary a data pre-processing before the training of ANN. To prepare good data for the learning algorithm, each input parameter is normalized using its standard deviation and the mean as eq. (7). For convenience in expressing the results, the output (factor of safety) is also mapped into the range of [0, 1] as eq. (8).

$$x_n = \frac{x-\mu}{\sigma}, \tag{7}$$

$$x' = \frac{x - x_{\min}}{x_{\max} - x_{\min}}, \tag{8}$$

where: x_n is the normalized value of x, μ and σ are the mean value and the standard deviation of each parameter, respectively; x' is the mapped value of x, x_{min} and x_{max} are the minimum and the maximum of the factor, respectively.

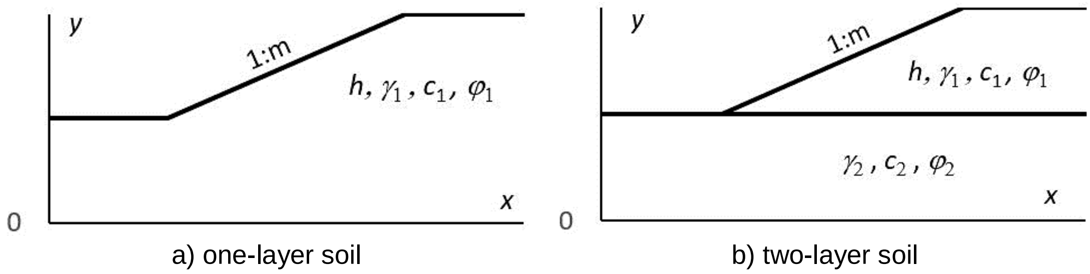

Fig. 4: Embankment configurations of two slope patterns.

Table 2: The slope parameters and factor of safety

Input parameters and output	One-layer soil	Two-layer soil
1. Slope height, *h* [m]	3, 4, 5, 6	3, 4, 5, 6
2. Slope ratio, *m*	1, 1.5, 2	1, 1.5, 2
3. Unit weight of layer 1, γ_1 [kN/m^3]	17, 18, 19	17, 18, 19
4. Cohesion of layer 1, c_1 [kN/m^2]	10, 15, 20	10, 15, 20
5. Internal friction angle of layer 1, φ_1 [°]	12, 15, 18, 21, 24	12, 15, 18, 21, 24
6. Unit weight of layer 2, γ_2 [kN/m^3]	-	16, 17, 18
7. Cohesion of layer 2, c_2 [kN/m^2]	-	5, 10, 15
8. Internal friction angle of layer 2, φ_2 [°]	-	6, 9, 12, 15, 18
Output: Factor of safety, *FS* (Fellenius' method)	min = 0.92, max = 3.98	min = 0.69, max = 3.31
Output: Factor of safety, *FS* (Bishop's method)	min = 0.97, max = 4.18	min = 0.75, max = 3.59
Total assessment cases	540	24300

Table 3. Examples of some results of slope stability

Configuration	*h* [m]	*m*	γ_1 [kN/m^3]	c_1 [kN/m^2]	φ_1 [°]	γ_2 [kN/m^3]	c_2 [kN/m^2]	φ_2 [°]	*FS* Fel./Bis.
One-layer soil	3	1	17	10	12	--	--	--	1.59/1.81
	4	1	18	15	21	--	--	--	2.01/2.17
	5	1.5	19	20	15	--	--	--	2.02/2.10
	6	2	18	10	15	--	--	--	1.39/1.47
Two-layer soil	3	1	17	10	24	16	5	6	1.11/1.17
	4	1	18	15	27	17	10	9	1.47/1.58
	5	1.5	19	10	27	16	15	6	1.28/1.42
	6	2	18	10	36	16	5	12	1.19/1.39

6 Results

For the whole 540 assessment cases of one-layer soil embankment, it can be seen that experimental data (target values on the horizontal axis) and values predicted by ANN (on the vertical axis) correlate well for both Fellenius' method in Fig. 5, and Bishop's method in Fig. 6, with the linear coefficient of correlation *R*, is around 0.99 in both training phase and testing phase. In addition, the ANN is applied for each slope height because of its significant effect on slope stability. The ANN predictions are also good for each slope height (135 cases for each slope height), with most of the correlation *R* being approximately 0.99 as shown in Fig. 7 for Fellenius' method and Fig. 8 for Bishop's method. The mean squared errors between the predicting outputs and the target values are very small, as given in Table 4.

For the two-layer soil embankment with a total of 240300 assessment cases, the correlation is even better with values of correlation *R* reaching almost 0.999 for both Fellenius' method in Fig. 9, and Bishop's method in Fig. 10. This remark is also the same for each wall height (with 60075 cases for each wall height) by Fellenius' method in Fig. 11, and Bishop's method in Fig. 12. The mean squared errors between the predicting outputs and the target values are also very small, as given in Table 5.

Table 4: The mean squared errors (MSE) for the embankments with one-layer soil.

Assessment case	All *H* = 3 m - 6 m	*H* = 3 m	*H* = 4 m	*H* = 5 m	*H* = 6 m
Fellenius' method (Training /testing phase)	0.0027 / 0.0017	0.0014 / 0.0016	0.0010 / 0.0025	0.0025 / 0.0031	0.0003 / 0.0005
Bishop's method (Training /testing phase)	0.0035 / 0.0037	0.0020 / 0.0061	0.0034 / 0.0048	0.0011 / 0.0043	0.0017 / 0.0109

Table 5: The mean squared errors (MSE) for the embankments with two-layer soil.

Assessment case	All *H* = 3 m - 6 m	*H* = 3 m	*H* = 4 m	*H* = 5 m	*H* = 6 m
Fellenius' method (Training /testing phase)	0.0007 / 0.0007	0.0005 / 0.0006	0.0004 / 0.0004	0.0003 / 0.0003	0.0003/ 0.0003
Bishop's method (Training /testing phase)	0.0008 / 0.0008	0.0006 / 0.0007	0.0005 / 0.0005	0.0004 / 0.0004	0.0003/ 0.0003

7 Conclusion

The study assessed the factor of safety of a large number of slope configurations using the differential evolution combined with limit equilibrium methods, then use them as a database for ANN performance. The ANN architecture, which is a multilayer perceptron model with the sigmoid activation function trained by the backpropagation learning algorithm using the gradient descent method, can predict very well the factor of safety of slopes in the experiment. The number of hidden layers and nodes for each slope pattern are chosen after the trial-and-error process to balance the quality of results and the running time. Although the study assessed a considerable number of slope cases, there is still a very large number of configurations needed to apply ANN for the prediction of the stability of any slope. However, the study showed the reliability of ANN in surveyed range of parameters. This can encourage accumulating more results of other slopes to enrich the database which makes ANN applicable for use in certain circumstances.

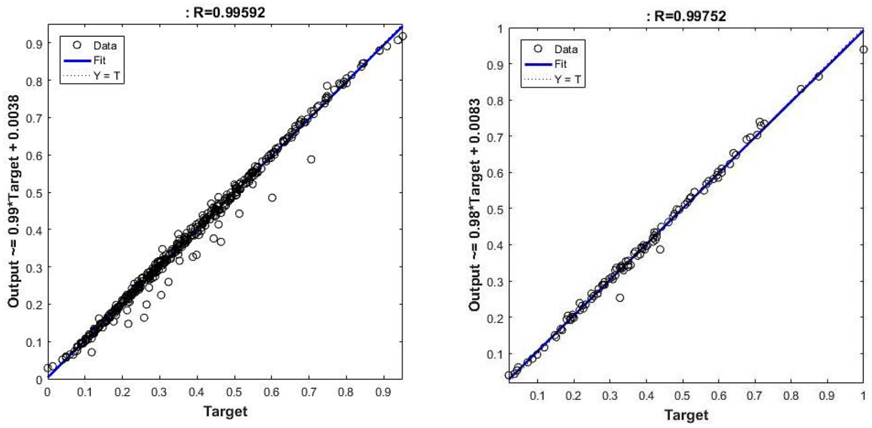

a) Training phase b) Testing phase

Fig. 5: ANN performance in prediction of factor of safety by Fellenius' method for one-layer soil embankment (for slope height *h* from 3 m to 6 m).

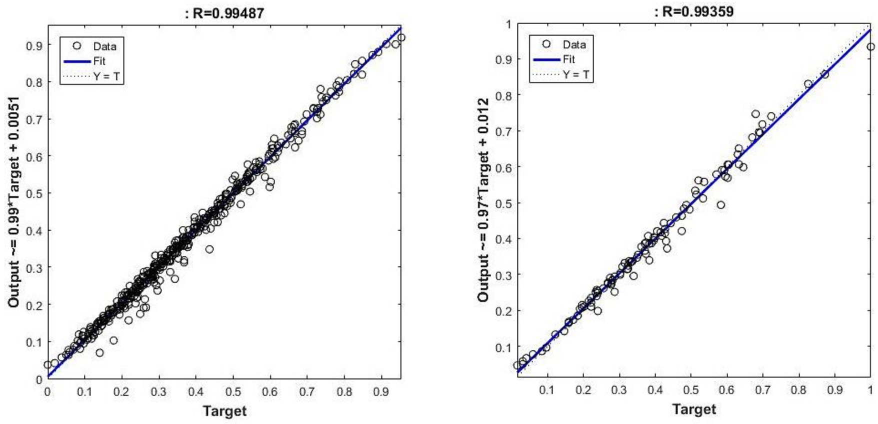

a) Training phase b) Testing phase

Fig. 6: ANN performance in prediction of factor of safety by Bishop's method for one-layer soil embankment (for slope height *h* from 3 m to 6 m).

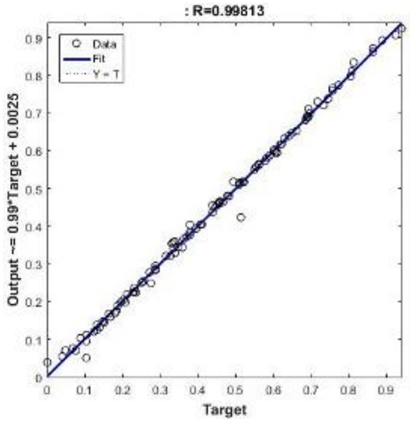

a) *h* = 3 m, Training phase

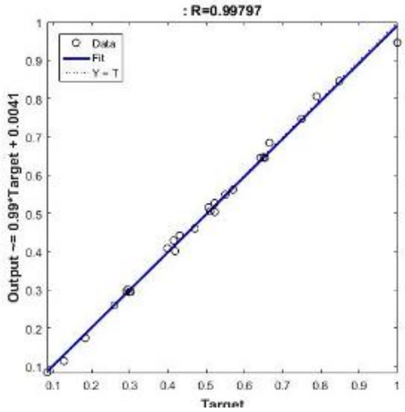

b) *h* = 3 m, Testing phase

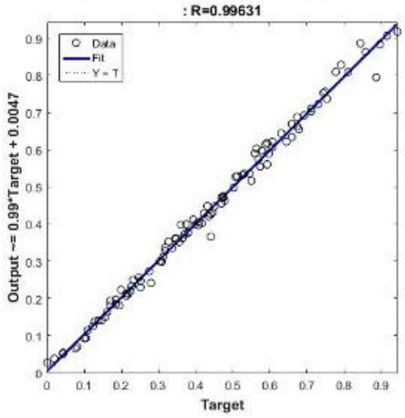

c) *h* = 4 m, Training phase

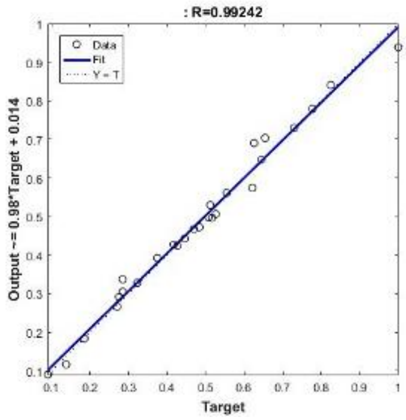

d) *h* = 4 m, Testing phase

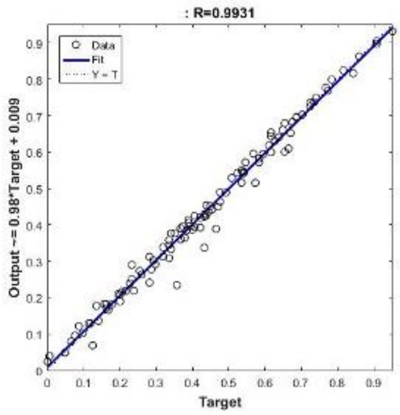

e) *h* = 5 m, Training phase

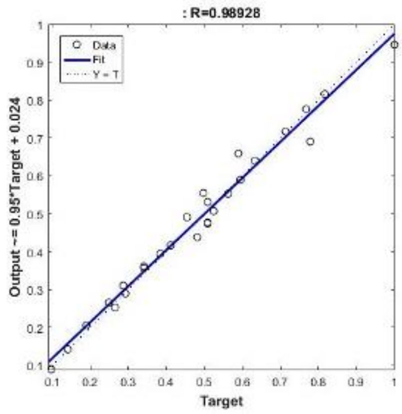

f) *h* = 5 m, Testing phase

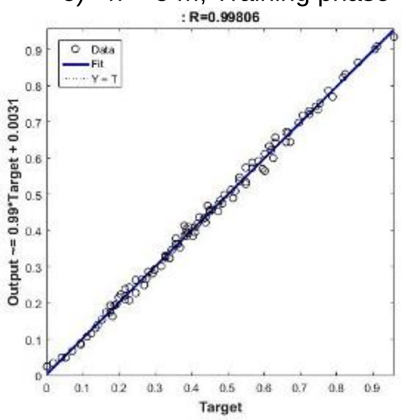

g) *h* = 6 m, Training phase

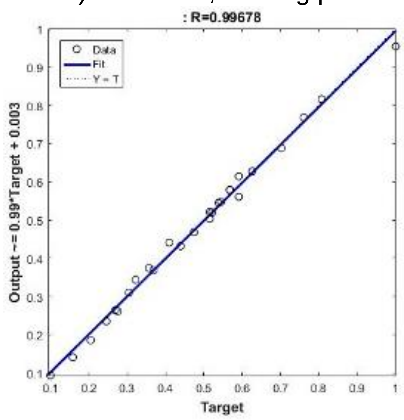

h) *h* = 6 m, Testing phase

Fig. 7: a) - h) ANN performance in prediction of factor of safety by Fellenius' method for one-layer soil embankment (for each slope height).

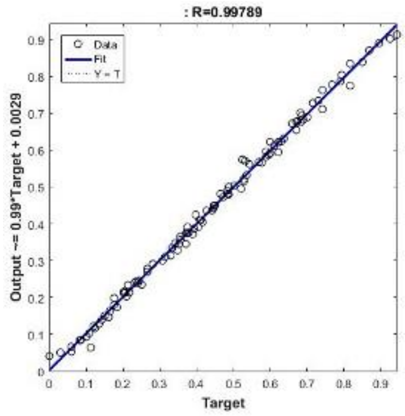

a) *h* = 3 m, Training phase

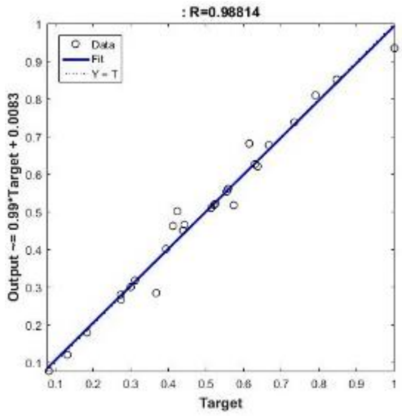

b) *h* = 3 m, Testing phase

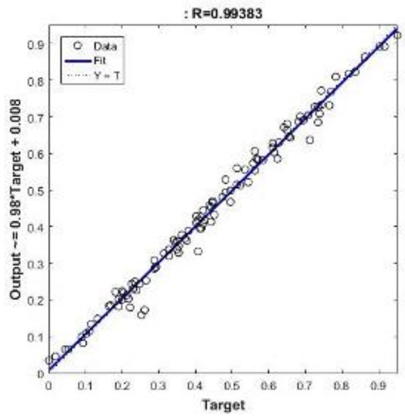

c) *h* = 4 m, Training phase

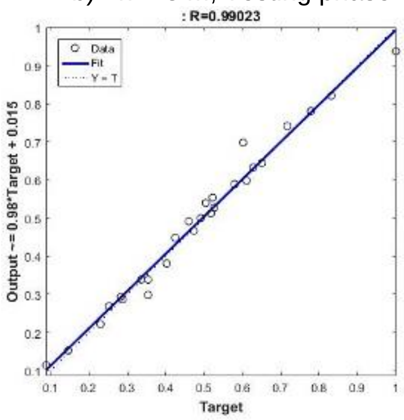

d) *h* = 4 m, Testing phase

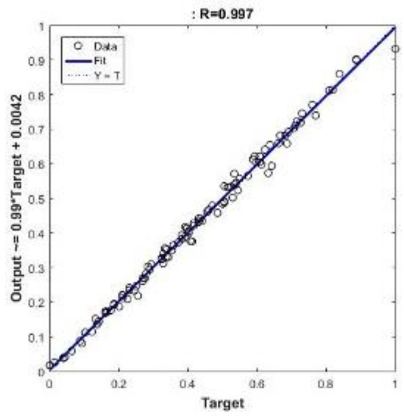

e) *h* = 5 m, Training phase

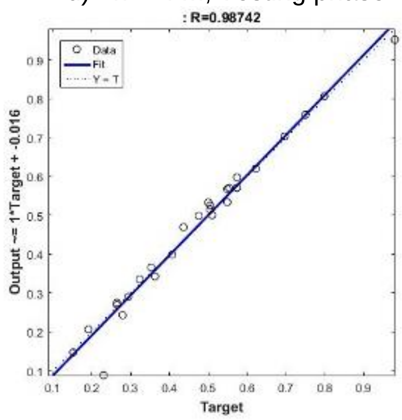

f) *h* = 5 m, Testing phase

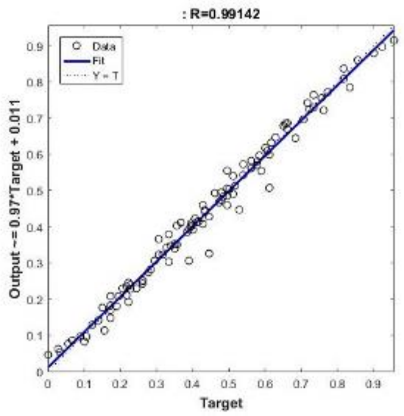

g) *h* = 6 m, Training phase

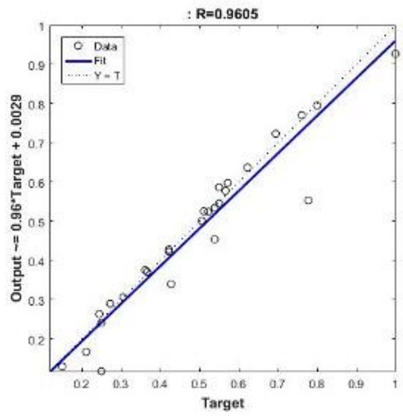

h) *h* = 6 m, Testing phase

Fig. 8: a) - h) ANN performance in prediction of factor of safety by Bishop's method for one-layer soil embankment (for each slope height).

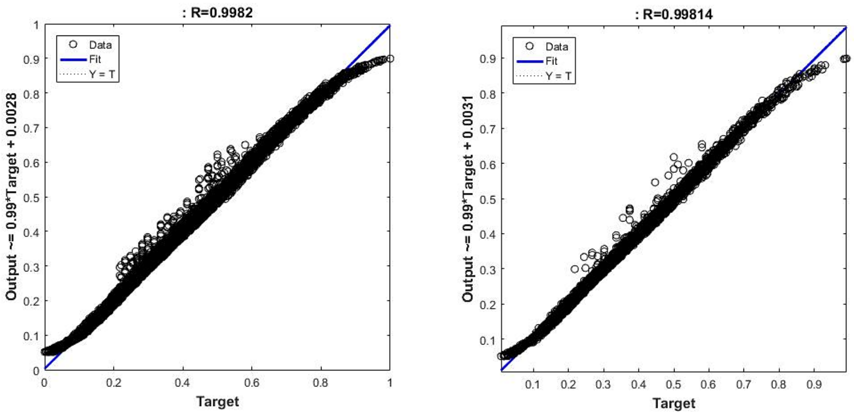

a) Training phase b) Testing phase

Fig. 9: ANN performance in prediction of factor of safety by Fellenius' method for two-layer soil embankment (for slope height *h* from 3 m to 6 m).

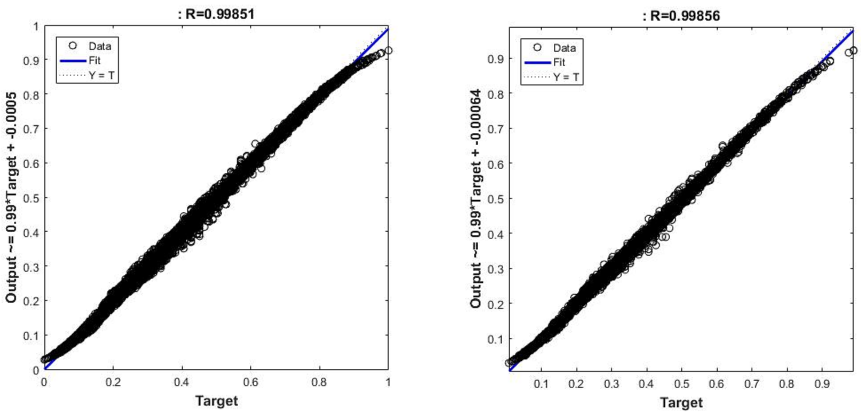

a) Training phase b) Testing phase

Fig. 10: ANN performance in prediction of factor of safety by Bishop's method for two-layer soil embankment (for slope height *h* from 3 m to 6 m).

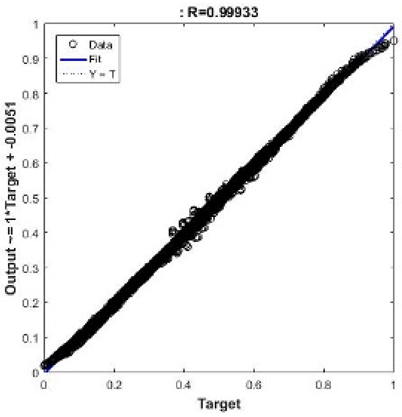

a) h = 3 m, Training phase

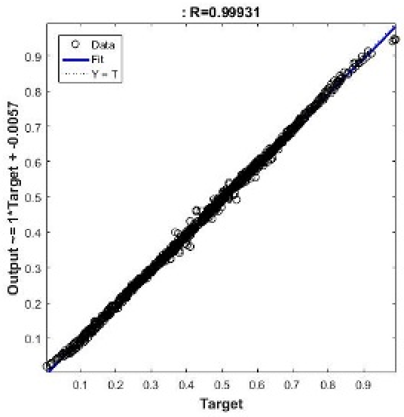

b) h = 3 m, Testing phase

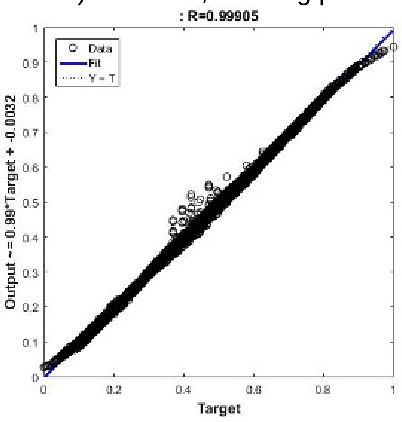

c) h = 4 m, Training phase

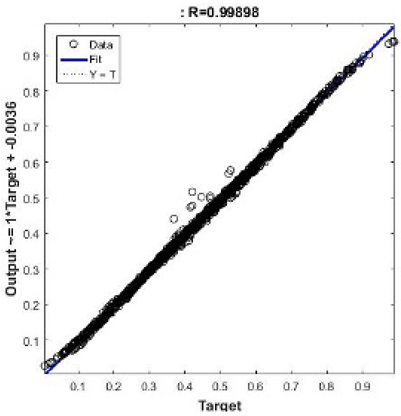

d) h = 4 m, Testing phase

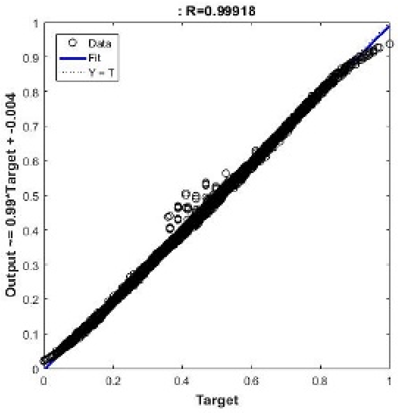

e) h = 5 m, Training phase

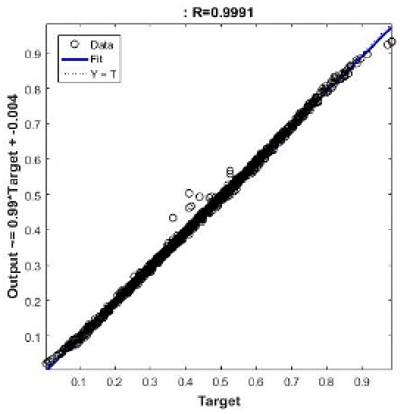

f) h = 5 m, Testing phase

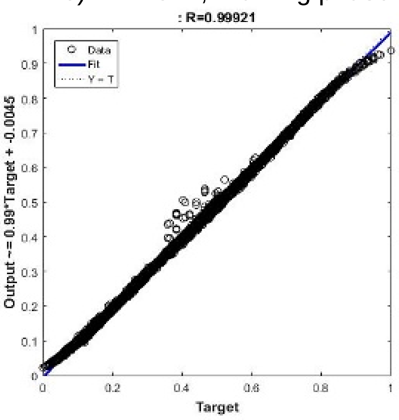

g) h = 6 m, Training phase

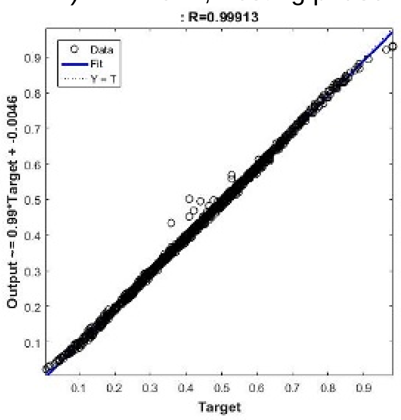

h) h = 6 m, Testing phase

Fig. 11: a) - h) ANN performance in prediction of factor of safety by Fellenius' method for two-layer soil embankment (for each wall height).

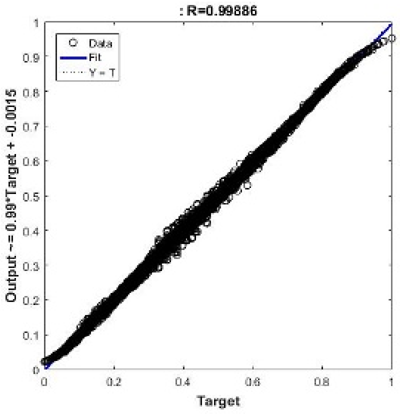

a) *h* = 3 m, Training phase

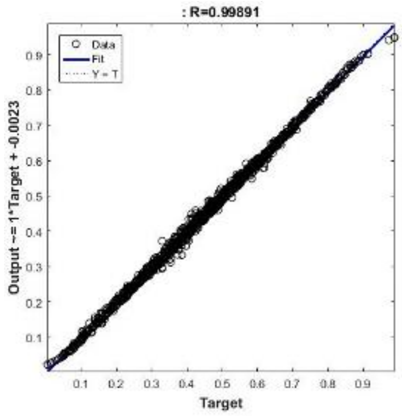

b) *h* = 3 m, Testing phase

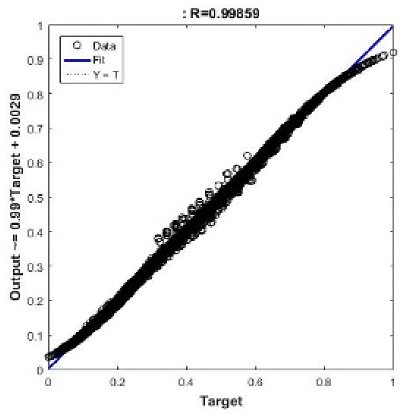

c) *h* = 4 m, Training phase

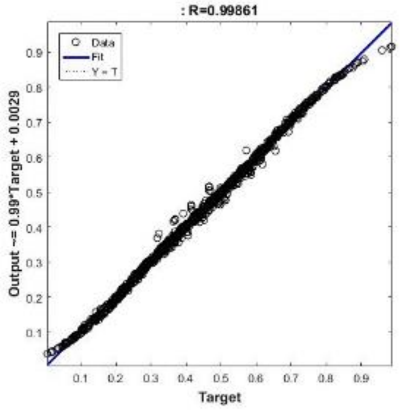

d) *h* = 4 m, Testing phase

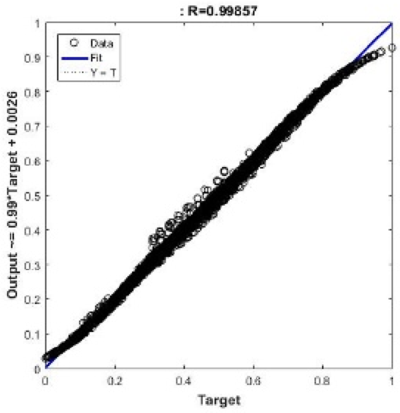

e) *h* = 5 m, Training phase

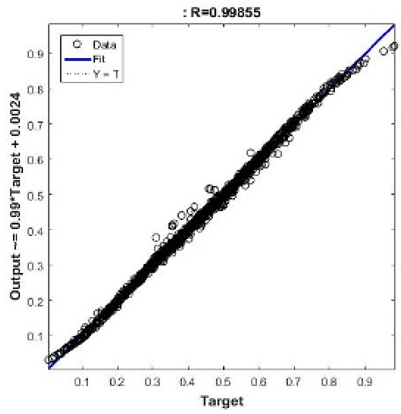

f) *h* = 5 m, Testing phase

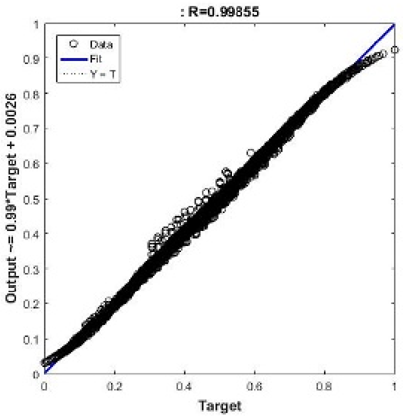

g) *h* = 6 m, Training phase

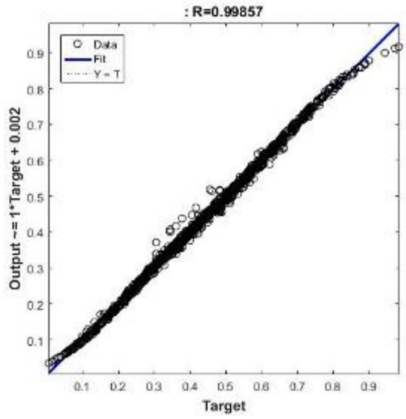

h) *h* = 6 m, Testing phase

Fig. 12: a) - h) ANN performance in prediction of factor of safety by Bishop's method for two-layer soil embankment (for each wall height).

References

[1] FELLENIUS, W.: Calculation of stability of earth dam. Transactions 2nd Congress Large Dams, Vol. 4 (7-8), 1936, pp. 445-462, Washington, DC.

[2] BISHOP, A. W.: The use of slip circle in the stability analysis of earth slopes. Geotechnique, Vol. 5, 1955, pp. 7-17.

[3] VU, V. T.: Evaluation of slope stability using method of slices with circular slip surfaces by genetic algorithms. Science and Technology Development Journal, Vol. 6 (7-8), 2003, pp. 110-115, https://doi.org/10.32508/stdj.v6i7&8.3352.

[4] GOH, A. T. C.: Search for critical slip circle using genetic algorithms. Civil Engineering and Environmental Systems, Vol. 17 (3), 2012, pp. 181-211.

[5] KAHATADENIYA, K. S. - NANAKORN, P. – NEAUPANE, K. M.: Determination of the critical failure surface for slope stability analysis using ant colony optimization. Engineering Geology, Vol. 108, 2009, pp. 133-141.

[6] KHAJEHZADEH, M. - TAHA, M. R. - El-SHAFIE, A. - ESLAMI, M.: Locating the general failure surface of earth slope using particle swarm optimization. Civil Engineering and Environmental Systems, Vol. 29 (1), 2012, pp. 41-57.

[7] VU, V. T.: Assessment of Slope Stability under Bounded Uncertainties Using Differential Evolution and Particle Swarm Optimization. Civil and Environmental Engineering, Vol. 18, Iss. 1, 2022, pp. 59-65, https://doi.org/10.2478/cee-2022-0006.

[8] SAKELLARIOU, M. G. – FERENTINOU, M. D.: A study of slope stability prediction using neural networks. Geotechnical and Geological Engineering, Vol. 23, 2005, pp. 419-445.

[9] QIAN, Z. G. – LI, A. J. – CHEN, W. C. – LYAMIN, A. V. – JIANG, J. C.: Artificial neural network approach to inhomogeneous soil slope stability predictions based on limit analysis methods, Soils and Foundations, Vol. 59, 2019, pp. 556–569.

[10] SAMUI, P.: Slope stability analysis: a support vector machine approach. Environmental Geology, Vol. 56, 2008, pp. 255–267, doi: 10.1007/s00254-007-1161-4.

[11] SAMUI, P. – KOTHARI, D. P.: Utilization of a least square support vector machine (LSSVM) for slope stability analysis. Scientia Iranica,Transactions A: Civil Engineering, Vol. 18(1), 2011, pp. 53-58, https://doi.org/10.1016/j.scient.2011.03.007.

[12] STORN, R. - PRICE, K.: Minimizing the real functions of the ICEC'96 contest by differential evolution. Proceedings of the IEEE Conference on Evolutionary Computation, 1996, pp. 842-844, Japan.

[13] RUMELHART, D. E. – HINTON, G. E. – WILLIAMS, R. J.: Learning internal representations by error propagation. Rumelhart DE, McClelland JL (Eds) Parallel distributed processing: Explorations in the microstructure of cognition, 1: Foundation, 1986, pp. 318–362. MIT Press, Cambridge.